Universiteit Leiden
The Netherlands

Optomechanical trampoline resonators

Kleckner, D.; Pepper, B.; Jeffrey, E.R.; Sonin, E.B.; Thon, S.M.; Bouwmeester, D.

Citation

Kleckner, D., Pepper, B., Jeffrey, E. R., Sonin, E. B., Thon, S. M., & Bouwmeester, D. (2011). Optomechanical trampoline resonators. *Optics Express*, *19*(20), 19708-19716. doi:10.1364/OE.19.019708

Version:	Not Applicable (or Unknown)
License:	Leiden University Non-exclusive license
Downloaded from:	https://hdl.handle.net/1887/65890

Note: To cite this publication please use the final published version (if applicable).

Optomechanical trampoline resonators

Dustin Kleckner,[1,2] Brian Pepper,[1] Evan Jeffrey,[3] Petro Sonin,[3] Susanna M. Thon,[1,4] and Dirk Bouwmeester[1,3,*]

[1] *Department of Physics, University of California, Santa Barbara, California 93106, USA*
[2] *Current address: The James Franck Institute, University of Chicago, Chicago, Illinois 60637, USA*
[3] *Huygens Laboratory, Leiden University, P.O. Box 9504, 2300 RA Leiden, The Netherlands*
[4] *Current address: Department of Electrical and Computer Engineering, University of Toronto, Toronto, Ontario M5S 3G4, Canada*
[*] *bouwmeester@physics.ucsb.edu*

Abstract: We report on the development of optomechanical "trampoline" resonators composed of a tiny SiO_2/Ta_2O_5 dielectric mirror on a silicon nitride micro-resonator. We observe optical finesses of up to 4×10^4 and mechanical quality factors as high as 9×10^5 in relatively massive (∼100 ng) and low frequency (10–200 kHz) devices. This results in a photon-phonon coupling efficiency considerably higher than previous Fabry-Perot-type optomechanical systems. These devices are well suited to ultra-sensitive force detection, ground-state optical cooling experiments, and demonstrations of quantum dynamics for such systems.

© 2011 Optical Society of America

OCIS codes: (230.1480) Bragg reflectors; (230.4000) Microstructure fabrication; (230.4685) Optical microelectromechanical devices.

References and links

1. A. Schliesser, O. Arcizet, R. Rivière, G. Anetsberger, and T. J. Kippenberg, "Resolved-sideband cooling and position measurement of a micromechanical oscillator close to the Heisenberg uncertainty limit," Nat. Phys. **5**, 509–514 (2009).
2. M. Eichenfield, J. Chan, R. M. Camacho, K. J. Vahala, and O. Painter, "Optomechanical crystals," Nature **462**, 78–82 (2009).
3. J. Chan, M. Eichenfield, R. Camacho, and O. Painter, "Optical and mechanical design of a "zipper" photonic crystal optomechanical cavity," Opt. Express **17**, 3802–3817 (2009).
4. L. Diósi, "Models for universal reduction of macroscopic quantum fluctuations," Phys. Rev. A **40**, 1165–1174 (1989).
5. R. Penrose, "On Gravity's role in Quantum State Reduction," Gen. Relativ. Gravit. **28**, 581–600 (1996).
6. D. Kleckner, I. Pikovski, E. Jeffrey, L. Ament, E. Eliel, J. van den Brink, and D. Bouwmeester, "Creating and verifying a quantum superposition in a micro-optomechanical system," New J. Phys. **10**, 095020 (2008).
7. I. Wilson-Rae, N. Nooshi, W. Zwerger, and T. J. Kippenberg, "Theory of Ground State Cooling of a Mechanical Oscillator Using Dynamical Backaction," Phys. Rev. Lett. **99**, 093901 (2007).
8. F. Marquardt, J. P. Chen, A. A. Clerk, and S. M. Girvin, "Quantum Theory of Cavity-Assisted Sideband Cooling of Mechanical Motion," Phys. Rev. Lett. **99**, 093902 (2007).
9. J. D. Teufel, T. Donner, D. Li, J. H. Harlow, M. S. Allman, K. Cicak, A. J. Sirois, J. D. Whittaker, K. W. Lehnert, and R. W. Simmonds, "Sideband Cooling Micromechanical Motion to the Quantum Ground State," ArXiv e-prints (2011).
10. J. Chan, T. P. M. Alegre, A. H. Safavi-Naeini, J. T. Hill, A. Krause, S. Groeblacher, M. Aspelmeyer, and O. Painter, "Laser cooling of a nanomechanical oscillator into its quantum ground state," ArXiv e-prints (2011).
11. D. Vitali, S. Gigan, A. Ferreira, H. R. Böhm, P. Tombesi, A. Guerreiro, V. Vedral, A. Zeilinger, and M. Aspelmeyer, "Optomechanical Entanglement between a Movable Mirror and a Cavity Field," Phys. Rev. Lett. **98**, 030405 (2007).
12. U. Akram, N. Kiesel, M. Aspelmeyer, and G. J. Milburn, "Single-photon opto-mechanics in the strong coupling regime," New J. Phys. **12**, 083030 (2010).

#150222 - $15.00 USD Received 6 Jul 2011; revised 19 Aug 2011; accepted 29 Aug 2011; published 23 Sep 2011

13. S. Bose, K. Jacobs, and P. L. Knight, "Scheme to probe the decoherence of a macroscopic object," Phys. Rev. A **59**, 3204–3210 (1999).
14. W. Marshall, C. Simon, R. Penrose, and D. Bouwmeester, "Towards Quantum Superpositions of a Mirror," Phys. Rev. Lett. **91**, 130401 (2003).
15. D. Kleckner, W. Marshall, M. J. A. de Dood, K. N. Dinyari, B.-J. Pors, W. T. M. Irvine, and D. Bouwmeester, "High Finesse Opto-Mechanical Cavity with a Movable Thirty-Micron-Size Mirror," Phys. Rev. Lett. **96**, 173901 (2006).
16. S. Gröblacher, K. Hammerer, M. R. Vanner, and M. Aspelmeyer, "Observation of strong coupling between a micromechanical resonator and an optical cavity field," Nature **460**, 724 (2009).
17. J. D. Thompson, B. M. Zwickl, A. M. Jayich, F. Marquardt, S. M. Girvin, and J. G. E. Harris, "Strong dispersive coupling of a high-finesse cavity to a micromechanical membrane," Nature **452**, 72–75 (2008).
18. S. Gröblacher, J. B. Hertzberg, M. R. Vanner, G. D. Cole, S. Gigan, K. C. Schwab, and M. Aspelmeyer, "Demonstration of an ultracold micro-optomechanical oscillator in a cryogenic cavity," Nat. Phys. **5**, 485–488 (2009).
19. A. M. Jayich, J. C. Sankey, B. M. Zwickl, C. Yang, J. D. Thompson, S. M. Girvin, A. A. Clerk, F. Marquardt, and J. G. E. Harris, "Dispersive optomechanics: a membrane inside a cavity," New J. Phys. **10**, 095008 (2008).
20. A. Nunnenkamp, K. Børkje, J. G. E. Harris, and S. M. Girvin, "Cooling and squeezing via quadratic optomechanical coupling," Phys. Rev. A **82**, 021806 (2010).
21. Mirrors were deposited by Coastline Optics, LLC, located in Camarillo, CA, USA.
22. A. Schliesser, R. Rivière, G. Anetsberger, O. Arcizet, and T. J. Kippenberg, "Resolved Sideband Cooling of a Micromechanical Oscillator," Nat. Phys. **4**, 415–419 (2008).
23. G. Cole, I. Wilson-Rae, M. Vanner, S. Gröblacher, J. Pohl, M. Zorn, M. Weyers, A. Peters, and M. Aspelmeyer, "Megahertz monocrystalline optomechanical resonators with minimal dissipation," in "Proc. IEEE Micr. Elect.," (2010), pp. 847–850.
24. D. Brodoceanu, G. D. Cole, N. Kiesel, M. Aspelmeyer, and D. Bauerle, "Femtosecond laser fabrication of high reflectivity micromirrors," Appl. Phys. Lett. **97**, 041104 (2010).
25. M. Li, W. H. P. Pernice, and H. X. Tang, "Reactive Cavity Optical Force on Microdisk-Coupled Nanomechanical Beam Waveguides," Phys. Rev. Lett. **103**, 223901 (2009).
26. D. Kleckner, W. T. M. Irvine, S. S. R. Oemrawsingh, and D. Bouwmeester, "Diffraction-limited high-finesse optical cavities," Phys. Rev. A **81** (2010).
27. M. Yamamoto, "Sub-nm figure error correction of an extreme ultraviolet multilayer mirror by its surface milling," Nucl. Instrum. Methods Phys. Res., A **467-468**, 1282–1285 (2001).
28. K. Kamijo, R. Uozumi, K. Moriziri, S. A. Pahlovy, and I. Miyamoto, "Two stage ion beam figuring and smoothening method for shape error correction of ULE substrates of extreme ultraviolet lithography projection optics: Evaluation of high-spatial frequency roughness," J. Vac. Sci. Technol. B **27**, 2900 (2009)
29. S. S. Verbridge, J. M. Parpia, R. B. Reichenbach, L. M. Bellan, and H. G. Craighead, "High quality factor resonance at room temperature with nanostrings under high tensile stress," J. Appl. Phys. **99**, 124304 (2006).
30. S. S. Verbridge, D. F. Shapiro, H. G. Craighead, and J. M. Parpia, "Macroscopic tuning of nanomechanics: substrate bending for reversible control of frequency and quality factor of nanostring resonators," Nano Lett. **7**, 1728–1735 (2007).
31. B. M. Zwickl, W. E. Shanks, A. M. Jayich, C. Yang, A. C. B. Jayich, J. D. Thompson, and J. G. E. Harris, "High quality mechanical and optical properties of commercial silicon nitride membranes," Appl. Phys. Lett. **92**, 103125 (2008).
32. M. Roseman and P. Grutter, "Cryogenic magnetic force microscope," Rev. Sci. Instrum. **71**, 3782–3787 (2000).
33. C. K. Law, "Interaction between a moving mirror and radiation pressure: A Hamiltonian formulation," Phys. Rev. A **51**, 2537–2541 (1995).
34. Q. Lin, J. Rosenberg, D. Chang, R. Camacho, M. Eichenfeld, K. J. Vahala, and O. Painter, "Coherent mixing of mechanical excitations in nano-optomechanical structures," Nat. Photonics **4**, 236–242 (2010).
35. A. A. Clerk, F. Marquardt, and J. G. E. Harris, "Quantum measurement of phonon shot noise," Phys. Rev. Lett. **104**, 213603 (2010).
36. H. J. Mamin and D. Rugar, "Sub-attonewton force detection at millikelvin temperatures," Appl. Phys. Lett. **79**, 3358–3360 (2001).
37. C. L. Degen, M. Poggio, H. J. Mamin, C. T. Rettner, and D. Rugar, "Nanoscale magnetic resonance imaging," Proc. Natl. Acad. Sci. USA **106**, 1313–1317 (2009).

---

1. Introduction

Optomechanical systems offer a potential avenue for observing quantum effects in mesoscopic systems. Although integrated micro-optomechanical systems like microtoroids [1] and optomechanical crystals [2, 3] have demonstrated a large degree of optomechanical coupling, their relatively small mass and high frequencies make them unattractive for probing mass-induced

#150222 - $15.00 USD Received 6 Jul 2011; revised 19 Aug 2011; accepted 29 Aug 2011; published 23 Sep 2011
(C) 2011 OSA

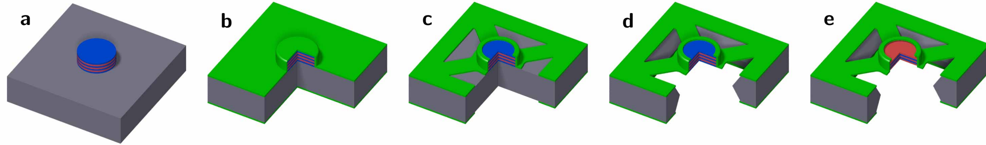

Fig. 1. The main steps in the fabrication process, carried out on a silicon wafer (gray). **a)** The process begins with the deposition of the SiO_2 (blue) / Ta_2O_5 (pink) dielectric mirror, which is then etched into discs of the desired size (only 7 of the 33 dielectric layers are shown). **b)** Si_3N_4 (green) is deposited on both sides of the wafer. **c)** The front side Si_3N_4 is etched into the resonator geometry and the backside has square holes etched for the Si etch. **d)** The carrier wafer is etched through with a TMAH anisotropic etch, releasing the resonators. **e)** A short BHF etch strips the protective SiO_2 layer off the front of the mirror, and the sample is then removed from solution with a critical point dry.

decoherence [4–6]. Here we describe the fabrication and operation of low frequency optomechanical "trampoline" resonators composed of a tiny SiO_2/Ta_2O_5 dielectric mirror on a silicon nitride micro-resonator. This combines the ideal mechanical properties of tensed Si_3N_4 resonators with the best available optical mirrors. The demonstrated systems have extraordinarily high mechanical quality factors and a photon-phonon coupling ratio comparable to the best integrated devices. If operated at cryogenic temperatures, these devices are well suited to ultra-sensitive force detection, ground-state optical cooling experiments [7–10], demonstrations of quantum effects [11, 12], and potentially even the realization of macroscopic quantum superpositions [6, 13, 14] with continued improvement in optical quality.

There have been several past realizations of optomechanical systems made from a tiny mirror on a mechanical resonator, for example, pieces of dielectric mirror glued to commercial AFM cantilevers [15] or deposited on top of a high frequency (MHz) Si_3N_4 resonator [16]. The combination of low optical and mechanical losses make Si_3N_4 an ideal mechanical material for this application; for tensed Si_3N_4 in particular the mechanical loss is typically observed to improve by an order of magnitude or more at the cryogenic temperatures required for quantum optomechanical experiments [17, 18]. The previously demonstrated mirror on Si_3N_4 systems had low mechanical quality factor, due to their high frequency and resulting clamping loss. Using an alternate fabrication method, we show that it is possible to increase the quality factor and make resonators at much lower mechanical frequencies. Furthermore, due to our unique undercutting method, our device allows free-space optical access to both sides of the mirror. This would make it ideal for "membrane in the middle" type optomechanical systems which would benefit greatly from the enhanced reflectivity of a dielectric mirror as compared to the single layer dielectric resonator that has been used previously [17], particularly if operating in the quadratic coupling regime [19, 20].

2. Fabrication of the system

The micro-optomechanical element is fabricated using standard cleanroom procedures (Fig. 1). We begin with a commercially deposited [21] dielectric mirror on a thin silicon (100 μm thick) wafer. This mirror is etched into disks of diameter 30–80 μm. We then deposit Si_3N_4 on both sides of the wafer, with a thickness in the range $t = 300$–500 nm. The front side Si_3N_4 is patterned into a cross resonator geometry (Fig. 2) with a diagonal length of $a = 250$–2000 μm and arm width of $w = 2$–30 μm. The back side of the wafer is patterned with a square hole to match the front side of the wafer. The wafer is then etched through with a silicon anisotropic etch (10% TMAH at 85° C), which releases the mechanical resonators with minimal undercutting of the Si_3N_4 where the structure connects to the bulk. Finally, the exposed layers of the dielec-

#150222 - $15.00 USD Received 6 Jul 2011; revised 19 Aug 2011; accepted 29 Aug 2011; published 23 Sep 2011
(C) 2011 OSA

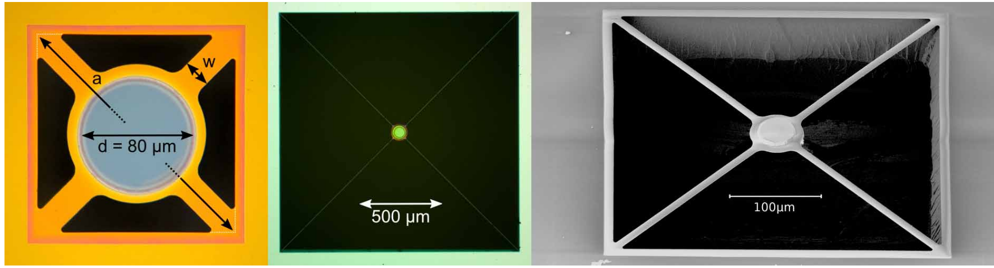

Fig. 2. Three micro-optomechanical resonators, as viewed from the top of the carrier wafer. Left: optical image, diameter $d = 80$ μm, Si_3N_4 of thickness $t = 500$ nm, with resonator arms of diagonal length $a = 250$ μm and width $w = 20$ μm. Center: optical image, $d = 80$ μm, $t = 300$ nm, $a = 2000$ μm, $w = 2$ μm. Right: scanning electron microscope image, $d = 40$ μm, $t = 500$ nm, $a = 500$ μm, $w = 10$ μm. Note that the anisotropic etch profile of TMAH is clearly visible in the silicon at the top of the image.

tric mirror, composed of SiO_2, are stripped with a short BHF etch; after this step the previously protected Ta_2O_5 layers form the new surfaces of the mirror.

We have also fabricated devices with Si_3N_4 resonators grown and etched before depositing the mirror layers. Although this method works, it has several disadvantages (including the fact that the roughness of the Si_3N_4 layer is then present on the mirror).

The other end of the optical cavity is a mirror with 50 mm radius of curvature and 15.9 mm outer diameter which was superpolished to better than 1 Å micro-roughness. The separation of the two mirrors is slightly (1-3 μm) shorter than the radius of curvature of the large mirror. This is required for a tight focus on the small mirror with a typical beam radius of 10 μm on a 60 μm diameter mirror. This gives a 1.6 mm beam radius on the large mirror and requires approximately 1 cm of clear aperture to minimize diffraction losses on both mirrors. In order to match the reflectivity of the optomechanical devices to the macroscopic end mirrors, the dielectric coating was deposited in the same run. The transmission of the coating was measured by the manufacturer to be 60 ± 10 PPM on the large mirror substrate at the design wavelength ($\lambda = 1064$ nm). The two ends of the optical cavity are placed in a specially constructed mount with five motorized degrees of freedom. The whole cavity assembly is then inserted into a vacuum chamber fitted with windows for optical access.

3. Optical characterization

To characterize the optical quality of the trampoline resonators, we measure the ring-down time of the cavity formed with the large mirror (Fig. 3).

To measure the optical ringdown time, we first scan the length of the optical cavity by slightly more than half a wavelength of the Nd:YAG pump laser. When the cavity transmission rises above a certain threshold (set to about half of the fundamental mode peak height), a pulse generator is triggered which cuts off the laser intensity with an acousto-optical modulator (AOM). The switching time is less than 100 ns and the monitor avalanche photodiode amplifier has a bandwidth of 50 MHz, so the exponential decay of the cavity light is easily resolved provided $F \gtrsim 10^3$ (Fig. 3). Because this method provides a quick and robust measure of the cavity finesse, it is also used to fine tune the cavity alignment. The longest observed decay time was $\tau_{cav} = 2.11 \pm 0.02$ μs, corresponding to a finesse of $F = 39,800 \pm 400$. Finesses for several of our devices compared to several other optomechanical devices [2, 9, 15–17, 22–25] from the literature are found in Table 2. Although the maximum value was found for a cavity with an 80 μm tiny mirror, we routinely achieve finesses of greater than 3.5×10^4 for mirrors of 60 and

#150222 - $15.00 USD Received 6 Jul 2011; revised 19 Aug 2011; accepted 29 Aug 2011; published 23 Sep 2011
(C) 2011 OSA

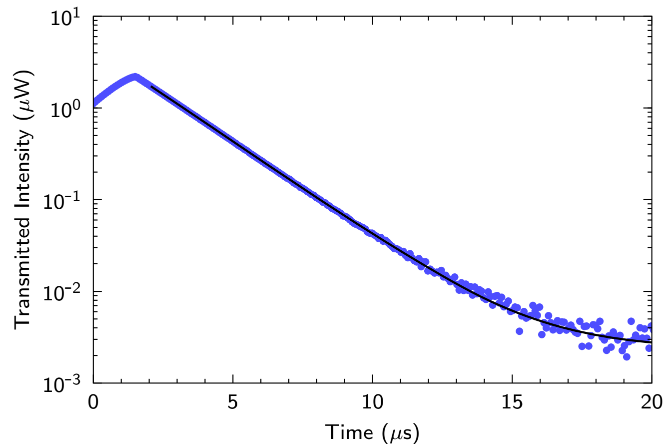

Fig. 3. The signal from the photodiode monitoring the cavity transmission during a typical optical ringdown measurement, showing the exponential decay of the signal after the pump laser is switched off via the AOM (averaged over 16 runs to reduce noise). Fitting the data starting 0.5 μs after the AOM switch results in an exponential decay time of $\tau_{cav} = 2.11 \pm 0.02$ μs.

80 μm diameter which have had the Si_3N_4 removed from the mirror region. By comparison, using two of the 15.9 mm mirrors in a confocal configuration resulted in an optical finesse of $F = 29,100 \pm 200$. The slightly higher finesse for the cavity with one tiny mirror is due to the fact that a dielectric mirror suspended in vacuum has higher reflectivity than one deposited on a glass substrate. (Samples with the resonator layer deposited first also show a slightly lower finesse, which then depends on the precise thickness of the Si_3N_4 dielectric layer.)

Samples with mirrors of 30 and 40 μm diameter are observed to have a lower cavity finesse, approximately 5×10^3 and 2×10^4, respectively. Although such a reduction might be expected from diffraction effects, theoretical studies indicate that in the absence of mirror imperfections the diffraction limited finesse of all devices should be considerably higher ($\gtrsim 10^6$) than the limitation imposed by the reflectivity of the dielectric mirrors [26]. The most likely source of imperfection is the wavefront error of our large mirror, which is on the order of several nm. This is consistent with the observed finesse, and suggests more sophisticated mirror polishing and surface figure correction techniques [27, 28] will be required for significant increase of the optical finesse, even with larger mirrors.

4. Mechanical characterization

To measure the intrinsic mechanical quality factor of the trampoline resonators, we monitor the motion of the tiny mirror with a laser locked to the fringe of a low finesse ($F \sim 100$) optical cavity. Depending on the frequency of the device in question, we determine the quality factor (Q_m) either by measuring the spectral linewidth or the mechanical decay time (see Fig. 4).

To measure the intrinsic mechanical quality factor of the resonators, we must first reduce the optical cavity finesse so that optical heating/cooling effects can be neglected. In practice this is most easily done by increasing the cavity length by a small amount ($\Delta L \sim 100$ μm) so that the beam no longer is able to tightly focus on the small mirror, increasing losses and decreasing finesse. We then lock the laser to the fringe of an optical resonance. To do this, we first modulate the laser frequency at a rate of 30 kHz with an amplitude of ~7.5 MHz. This generates 30 kHz harmonics in the transmitted intensity, as monitored on the photodiode at the output of the

#150222 - $15.00 USD   Received 6 Jul 2011; revised 19 Aug 2011; accepted 29 Aug 2011; published 23 Sep 2011
(C) 2011 OSA

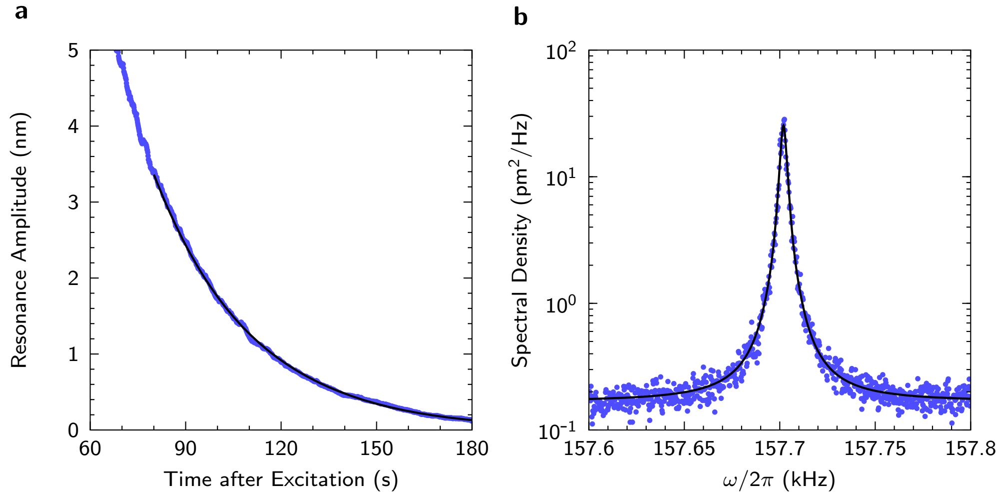

Fig. 4. **a)** The normalized amplitude of the fundamental mechanical resonance of a low frequency (9.174 kHz) resonator after it is excited by moving by one of the alignment motors by a single step. Data from the first minute after the excitation (not shown) is heavily distorted due to the mechanical amplitude becoming larger than the equivalent width of the optical peak ($\lambda/2F \sim 5$ nm). Fitting the data after $t = 80$ s results in a power decay time of $\tau = 15.4 \pm 0.3$ s, or a mechanical quality factor of $Q_m = (9.4 \pm 0.2) \times 10^5$. **b)** The thermal resonance spectrum of a high frequency ($\omega_m = 2\pi \times 157.7$ kHz) trampoline resonator. A fit to a Lorentzian gives a peak width (FWHM) of $\delta\omega_m = 2\pi \times 3.64 \pm 0.15$ Hz, corresponding to $Q_m = (4.3 \pm 0.2) \times 10^4$.

cavity. A lock-in amplifier measures the second harmonic of the modulation frequency, which is used as the input to an integrator circuit connected piezoelectric transducer which changes the cavity length. This locks the laser to the point of maximum slope on the optical fringe, resulting in an accurate measurement of the resonator's motion which is assumed to be much faster than the speed of the feedback loop (~ 1 Hz).

To measure the mechanical ring-down of low frequency resonators, we excite the system by moving one of the cavity alignment motors by a single 20 nm step. Due to the high frequency slip-stick motion of the motors, this causes a relatively large excitation ($\gtrsim 10$ nm) of the mechanical resonator whose decay time can easily be measured. Because the mechanical displacement can become comparable to or larger than the equivalent linewidth of the optical resonance, we use the fundamental harmonic (30 kHz) signal from the frequency modulation as a reference to linearize the fundamental mechanical amplitude signal. Although the ringdown provides a robust measure of mechanical quality, the excitation is large enough that it disturbs the locking of the pump laser to the cavity mode. Thus it can only be used for devices whose decay time is longer than the approximate locking time of the cavity feedback loop (~ 1 s); for higher frequency devices we instead measure the spectral linewidth of the thermally excited mechanical resonance.

We observe high mechanical quality factors for all devices, even at room temperature (see Table 2). For the lowest frequency device we measured a quality factor of $Q_m = (9.4 \pm 0.2) \times 10^5$ at $\omega_m = 2\pi \times 9.714$ kHz. In general, Q_m is highest for the lowest frequency devices, following an approximate $Q_m \propto \omega_m^{-1}$ trend, as is commonly seen in micromechanical systems [29, 30]. A slight deviation from this trend is seen for the highest frequency devices, in which case the stress relaxation induced by the mirror causes a moderate reduction in the tension of the resonator.

#150222 - $15.00 USD Received 6 Jul 2011; revised 19 Aug 2011; accepted 29 Aug 2011; published 23 Sep 2011
(C) 2011 OSA

In general, the quality factor of tensed Si_3N_4 resonators is observed to increase at cryogenic temperatures [18,31,32]. Using a preliminary cryogenic version of our optical cavity, we measured the Q_m at temperatures down to 300 mK. Using one of the higher frequency devices with frequency 157.7 kHz, we observed the quality factor to first increase as the device was cooled to 77 K. The Q_m increased to a maximum of 120,000 at 300 mK. The frequency and Q_m at various temperatures are displayed in Table 1. Although this increase is less than that of [31], this is likely due to the lower stress of our thin film.

Table 1. Dependence of frequency and quality factor on temperature as 157.7 kHz device is cooled to 300 mK with a dilution refrigerator.

T	$\omega_m/2\pi$ (kHz)	Q_m
300 K	159.0	20,000.
77 K	127.3	26,000.
4 K	122.8	40,000.
300 mK	122.8	126,000.

5. Prospects and conclusion

To analyze the suitability of trampoline resonators for quantum experiments, we need to characterize the degree of coupling between the optical and mechanical modes. The quantum hamiltonian of a standard optomechanical system is characterized by a linear optomechanical coupling rate, g, which couples the photon number of the optical mode to the position of the mechanical mode. For a Fabry-Perot cavity with one moving end mirror this coupling is given by [13, 33]:

$$g = \frac{\omega_c}{L} x_0, \tag{1}$$

where ω_c is the optical mode frequency, L is the cavity length and $x_0 = \left[\hbar / \left(2 m_{eff} \omega_m\right)\right]^{1/2}$ is the ground state wavepacket size of the mechanical mode (where m_{eff} is the effective mass of the fundamental mode). As a figure of merit, we will consider the product of the coupling rate, g, and the optical ring-down time, τ_{cav}:

$$g' = g\tau_{cav} = 2F\frac{x_0}{\lambda}. \tag{2}$$

This gives a dimensionless measure of how close a device is to being strongly coupled. (Note that coherent pumping can also make a weakly coupled device become strongly coupled: in this case an effective coupling is given by $g'_{eff} \approx \sqrt{\langle n \rangle} g'$ and $\langle n \rangle$ is the mean number of photons in the optical cavity [12, 16].) In the limit $g' \ll 1$ and $\omega_m \ll \tau_{cav}^{-1}$, g' gives the probability that a photon in the optical mode would excite the mechanical resonator out of the ground state. A comparison of the optical and mechanical quality of trampoline resonators to other optomechanical systems is shown in Table 2. The mass of our resonator is calculated from the mirror geometry.

We find the our devices have an optomechanical coupling efficiency nearly equal to the best integrated optical devices (microtoroids), despite having an order of magnitude larger mass. We are also within an order of magnitude of the best reported RF devices [9]. If the finesse could be increased to the theoretical diffraction limited value it should be possible to create devices with considerably higher optomechanical coupling than any current device. The finesse increases exponentially with the number of layers so can be increased dramatically with only

#150222 - $15.00 USD Received 6 Jul 2011; revised 19 Aug 2011; accepted 29 Aug 2011; published 23 Sep 2011
(C) 2011 OSA

Table 2. A comparison of trampoline resonators with other previously demonstrated optomechanical systems.

	m_{eff} (ng)	$\omega_m/2\pi$ (kHz)	Q_m	F	$g' \times 10^6$
Trampoline resonators:					
Device 1[a]	110	9.71	940,000	29,000*	150
Device 2[b]	60	46.2	190,000	35,000	115
Device 3[c]	60	157.7	43,000	38,000	67
Other optomechanical systems:					
Al drum/microwave cavity [9]	0.048	10,560	330,000	37,700†	997
Microtoroid [22]	10	40,600	31,200	155,000	200
Optomechanical crystal [2]	0.0003	2,250,000	1,280	38,000†	44
GaAs/AlGaAs bridge [23]	3.4	3,840	80,000	26,000	39
Double disk [34]	0.26	8,300	4‡	691,000†	37
Si_3N_4 membrane in cavity [17]	40	134	1,100,000	15,200	30
Mirror on AFM cantilever [15]	24	12.5	137,000	2,100	21
Mirror on Si_3N_4 bridge [16]	145	974	6,700	14,000	6.5
Dielectric mirror bridge [24]	50	350	6,000	8,900	3.7
Microdisk/waveguide [25]	0.0009	25,400	5,000	740	0.02

Note that in some cases the listed parameters were inferred from other published quantities, and all values should be regarded as approximate. Also note that g' is calculated using the appropriate formula for each type of device; Eqn. 2 applies only to Fabry-Perot optical cavities with one moving end mirror.

[a]Dimensions $a = 2$ mm, $w = 2$ μm, $t = 300$ nm, $d = 80$ μm

[b]Dimensions $a = 1$ mm, $w = 10$ μm, $t = 300$ nm, $d = 60$ μm

[c]Dimensions $a = 0.35$ mm, $w = 30$ μm, $t = 500$ nm, $d = 60$ μm

*The Si_3N_4 was not removed from the mirror region for this resonator, resulting in a slightly lower finesse.

†F is not clearly defined for these devices; the optical quality factor is listed instead.

‡This is the Q of the optically coupled flapping mode. The breathing mode has higher Q=124.

minor mass increase. The main limitation is then wavefront error which must be improved before substantially lower loss coatings can effectively be used.

This high degree of optomechanical coupling of trampoline resonators makes them ideal for demonstrations of quantum effects in massive systems. A first step towards demonstrating quantum effects is ground state optical cooling, which also requires low initial temperature and a "sideband-resolved" mechanical resonance [7, 8]. In particular, the bath temperature of the resonator must be low enough that [7, 8]:

$$Q_m \gg \frac{1}{\exp(\frac{\hbar\omega_m}{k_B T}) - 1} \tag{3}$$

In the $k_B T \gg \hbar\omega_m$ regime, this simplifies to:

$$T \ll Q_m \frac{\hbar\omega_m}{k_B}. \tag{4}$$

For our devices, this corresponds to $T \ll 0.5$ K. Although we have already demonstrated base temperatures in this regime, there are significant experimental challenges with aligning a high quality optical cavity at these temperatures. The sideband-resolved requirement is that the optical decay rate be smaller than the mechanical resonance frequency, $\tau_{cav}^{-1} < \omega_m$ which is met for our devices with $\omega_m \gtrsim 2\pi \times 80$ kHz, provided the sample finesse can be achieved in cryogenic

#150222 - $15.00 USD Received 6 Jul 2011; revised 19 Aug 2011; accepted 29 Aug 2011; published 23 Sep 2011
(C) 2011 OSA

conditions. If ground state optical cooling can be achieved, this opens the door to a number of other demonstrations of quantum effects [6, 14, 17, 19, 35].

Trampoline resonators are also suitable for use as ultra-high resolution force sensors. Assuming the quality factor increase is also seen for the lowest frequency devices, it should be possible to obtain a thermal force noise in the $\mathrm{aN}/\sqrt{\mathrm{Hz}}$ regime at demonstrated temperatures. This is comparable to or better than the single crystal Si resonators currently used in magnetic resonance force microscopy (MRFM) experiments [36, 37]. Furthermore, the rear side optical access can be used to provide extremely precise position sensitivity while leaving the front side free for surface modifications required for use as sensors.

In conclusion, we have demonstrated the development of low frequency micro-optomechanical systems with an extraordinarily high optical and mechanical quality by combining the best properties of previous systems in a single device. Due to their ideal properties, including the highest published photon-phonon coupling efficiencies for optical Fabry-Perot type systems, and unique double sided optical access, these devices are well suited for both practical applications and demonstrations of quantum effects with mesoscopic objects.

Acknowledgments

The authors gratefully acknowledge support by the National Science Foundation (grant PHY-0504825 and NIRT grant 0304678), Marie-Curie EXT-CT-2006-042580, the U.S. Department of Education GAANN grant, European Commission Project MINOS, and the NWO VICI award. A portion of this work was done in the UCSB Nanofabrication Facility, part of the NSF-funded NNIN network.

#150222 - $15.00 USD Received 6 Jul 2011; revised 19 Aug 2011; accepted 29 Aug 2011; published 23 Sep 2011
(C) 2011 OSA